Advancements in Nanostructured Electron Acceptors

Dr. Kavita Patel, Prof. Rohan Desai

Indian Institute of Technology, Mumbai, India

Abstract—Zinc sulphide (ZnS) quantum dots (QDs) were synthesized successfully via simple sonochemical method. X-ray diffraction (XRD), scanning electron microscopy (SEM) and high resolution transmission electron microscopy (HRTEM) analysis revealed the average size of QDs of the order of 3.7 nm. The band gap of the QDs was tuned to 5.2 eV by optimizing the synthesis parameters. UV-Vis absorption spectra of ZnS QD confirm the quantum confinement effect. Fourier transform infrared (FTIR) analysis confirmed the formation of single phase ZnS QDs. To fabricate the diode, blend of ZnS QDs and P3HT was prepared and the heterojunction of PEDOT:PSS and the blend was formed by spin coating on indium tin oxide (ITO) coated glass substrate. The diode behaviour of the heterojunction was analysed, wherein the ideality factor was found to be 2.53 with turn on voltage 0.75 V and the barrier height was found to be 1.429 eV. ZnS-Graphene QDs nanocomposite was characterised for the surface morphological study. It was found that the synthesized ZnS QDs appear as quasi spherical particles on the graphene sheets. The average particle size of ZnS-graphene nanocomposite QDs was found to be 8.4 nm. From voltage-current characteristics of ZnS-graphene nanocomposites, it is observed that the conductivity of the composite increases by 10^4 times the conductivity of ZnS QDs. Thus the addition of graphene QDs in ZnS QDs enhances the mobility of the charge carriers in the composite material. Thus, the graphene QDs, with high specific area for a large interface, high mobility and tunable band gap, show a great potential as an electron-acceptors in photovoltaic devices.

Keywords—Graphene, mobility, nanocomposites, photovoltaics, quantum dots, zinc sulphide.

I. Introduction

In recent decades, organic photovoltaics based on conjugated polymer and semiconductor QDs have attracted more attention. To fulfill the increasing demand of clean energy, conversion of solar energy into electrical energy at economically viable cost is needed [1]-[4]. Bulk heterojunctions (BHJ) based on the blends of conjugated polymer donors and inorganic acceptors are one of the most promising candidates for the fabrication of low-cost solar cells to meet the clean-energy demands of the 21st century. This type of solar cells possesses unique advantages of the both the components such as low-temperature processing of organic semiconductors and high dielectric constant of inorganic semiconductors. QDs (e.g., CdSe, CdTe, PbTe, PbS) are

emerging as the leading acceptor materials in photovoltaics 3,4 due to their size-tuned optical response, efficient multiple carrier generation, and low cost. QD solar cell brought the revolution in photovoltaics owing to their quantum confinement effect, their tuned band gap that allows to absorb entire gamut of sunlight (from UV to IR), multiple exciton generation efficiency etc. [5], [6]. The crucial task in developing high performance QD solar cell is the effective dissociation of excitons and transfer of these carriers to their respective electrodes. Recently, it was reported that a newly emerging material, graphene quantum dots (GQDs) is useful for optoelectronic applications due to its tunable band gap which in turn depends on its size and chemical functionality, which is important to improve the efficiency of the optoelectronic devices [7], [8]. Carbon nanostructures, due to their unique and novel properties, have generated potential applications in QD solar cells [9], [10]. Particularly, SWNTs and stacked-up carbon nanotubes have been used as efficient acceptors to enhance photoinduced charge transfer for improved performance because of their unique onedimensional nanostructure and appropriate band energy [11][13].

Graphene, a 2D sheet composed of sp 2-bonded single-layer carbon atoms with the honeycomb lattice structure, has attracted great research interest in physics, chemistry, materials science, etc. Its extremely high room-temperature carrier mobility (≈20 000 $cm^2 v^{-1} s^{-1}$) makes graphene a promising candidate to replace the conventional semiconductor materials in the electric circuit [14]. Higher carrier mobility means that charges are transported to respective electrodes more quickly, which reduces current losses via recombination and therefore improves the efficiency of a solar cell. Moreover, the high optical transparency of graphene (only 2.3% of incident light absorbed in the range from near-infrared to violet) makes it promising for nextgeneration transparent conductive electrodes, which may replace traditional ITO in optoelectronics, displays, and photovoltaics [15]. Lots of impressive results have been reported [16], where graphene was used as the electrodes, i.e., transparent & non-transparent anodes, transparent cathodes and catalytic counter electrodes etc. Uses of graphene as an active layer, for example light harvesting material, Schottky junction, electron and hole transport layer as well as interfacial layer in the tandem configuration are also reported [17]. In addition, graphene shows much better mechanical flexibility than ITO and metal electrodes. Therefore, it is suitable for the applications in flexible electronics. However, the easy aggregation and the poor dispersion of 2D graphene sheets in common solvents limit its application in such devices. Although effort has been made to prepare solution-processable functionalized graphenes (SPFGs), the non-uniform size and shape, on a scale of several hundred nanometers and even micrometers of SPFGs, remain big challenges for the fabrication of high performance photovoltaic cells with active layer thicknesses of only nanometer scale [7]. To facilitate the application of graphene in nanodevices and to effectively tune the

bandgap of graphenes, a promising approach is to convert the 2D graphene sheets into 0D GQDs [16]-[22].

A. Graphene as Transparent Conducting Anode

Graphene is used as a transparent conducting anode in organic photovoltaic device with composition PET/rGO/ PEDOT:PSS/P3HT:PCBM/TiO_2/Al with the transparency of 65%. The CVD grown graphene as anode in quartz/graphene/ PEDOT:PSS/CuPc:C60/BCP/Ag cell shows the efficiency of 0.85%. PET/graphene/PEDOT:PSS/CuPc:C60/BCP/Al shows increase in efficiency of 1.18% with 89% transparency. The flexible photovoltaics shows better performance with quartz/ graphene/MoO_3:PEDOT:PSS/P3HT:PCBM/LiF/Al as compared to ITO substrates. It gives efficiency of 2.5% and transparency of 90%. The photovoltaic device with configuration of Au-graphene/PEDOT:PSS/P3HT:PCBM/ ZnO/ITO shows graphene as transparent electrode with efficiency 3.04% [23]-[39].

B. Graphene as Transparent Conducting Cathode

In the hybrid solar cell with configuration Quartz/rGO/ ZnO/P3HT/PEDOT:PSS/Au, graphene was used as a transparent cathode with 61% transparency and shows an efficiency of 0.31% and CVD grown graphene in hybrid device glass/graphene/PEDOT:PEG(PC)/ZnO/PbS QD(P3HT)/MoO 3/Au shows 4.2% efficiency. The Au/ graphene/Al-TiO 2/P3HT:PCBM/MoO 3/Ag flexible organic photovoltaics show 2.58% efficiency with 96%transparency. CVD synthesized graphene shows 4.17% efficiency in thin film solar cell: Glass/graphene/ZnO/CdS/CdTe/graphite paste [40]-[42].

C. Graphene Used in Active Layers

Various methods have been used for the functionalization of graphene. The solution processed functionalized graphene was used to synthesize poly(3-octylthiophene):graphene composite blend for active layer in BHJ device. The ITO/ PEDOT:PSS/P3OT:graphene/LiF/Al cell has achieved the power conversion efficiency of 1.4% by using the graphene as electron acceptor material. In the active layer of ITO/P3HT/ ANI-GQDs/Al photovoltaic device, P3HT acts as a donor material and aniline functionalized GQDs as an acceptor achieves an efficiency of 1.14%.

Solar cells based on Schottky junctions between graphene sheets and CdSe has been designed with configuration of Si/ SiO_2/graphene-CdSe nanobelt/In-Au. An ideal Schottky junction facilitates the electron-hole separation and diffusion driven by the built-in potential between graphene and semiconductor. It shows the open-circuit voltage of 0.51 V, a short-circuit current density of = 5.75 mA cm^{-2} and an overall power conversion efficiency of 1.25% has been obtained. Bis(Trifluoromethanesulfonyl-amide) (TFSA) doped graphene has lower sheet resistance. TFSA increases the work function of graphene, thus increasing the built-in potential between the doped-graphene and n-Si in solar cells. The Schottky junction solar cell In/Ga eutectic/n-Si/TFSA doped graphene/Cr/Au increases the efficiency from 1.9% to 8.6% after doping with TFSA [43]-[46].

Due to the high electron mobility, graphene can be used as a transport material in solar cell. In BHJ solar cell of configuration ITO/PEDOT:PSS/P3HT:PDI-graphene/LiF/Al, graphene was used as an electron transport layer and achieves an efficiency of 1.04%. In the organic photovoltaic device of ITO/PEDOT:PSS/PCDTBT/PC71BM/GO/TiO_2/Al, graphene was first functionalized by using nitric acid and sulphuric acid and achieves an efficiency of 7.5. The hole blocking layer of graphene oxide enables the photogenerated electron towards the Al electrode. It enhances short circuit current density and power conversion efficiency [35].

In organic photovoltaics of ITO/GO/P3HT:PCBM/Al, GO acts as hole transport layer showing enhanced PCE 3.5% as compared to the ITO/PEDOT:PSS/rGO-P3HT/C60/Al device with 0.61% efficiency. To reduce the resistance in polymer solar cell, reduced graphene oxide (rGO) was used as a hole transport layer. *p*-toluenesulfonyl hydrazide was used to reduce GO. The device ITO/r-GO/P3HT:PCBM/Ca/Al with rGO shows the increased PCE of 3.7%. Huang et al. [36], [37] have used the GO and SWCNT as a hole transport layer in configuration of ITO/GO-SWCNT/P3HT:PCBM/Ca/ Al polymer solar cell. The addition of SWCNT in GO increases the conductivity of GO film. The composite film decreases the hole transport resistance and increases the efficiency by 4.1% as compared to simple GO device.

GO can be used as hole as well as electron transport material. The work function for pure GO is 4.6–4.8 eV and it can be reduced to 3.9–4.1 eV by changing the COOH group in GO with COOCs groups (cesium neutralized GO). The device ITO/GO/P3HT:PCBM/GOCs/Al shows the PCE of 3.67% as GO work function matches with ITO and P3HT and COOCs work function matches with PCBM and Al [47]-[50].

II. Experimental

A. Synthesis of Zns-Graphene Nanocomposites

Graphene was covalently functionalized by acidic treatment. Graphene was added to the mixture of sulphuric and nitric acid in the ratio 3:1. The mixture was ultrasonicated for homogenous solution and then it was diluted with deionized water. The mixture was centrifuged for 5 min and washed many times with water. The precipitate was dried at 100 °C, that gives the functionalized graphene.

The functionalized graphene was dispersed in deionized water by ultrasonication. Equimolar zinc acetate and thioacetamide was mixed thoroughly in water. After complete mixing, both the solutions mixed together by stirring and ultrasonication process for 2 hrs. The precipitate was collected by centrifugation. The product was washed many times with water and ethanol, annealing was done at 60 °C. The dried product gives the ZnS-graphene nanocomposites.

B. Characterization

The material was structurally characterized by XRD using X'pert-Pro (PANalytical) diffractometer with CuK_α radiation (λ=1.5406 Å). Surface morphology of ZnS-graphene particles was observed with the help of FEG-SEM (Hitachi, S-4800). The composition of the sample was measured by EDX spectrometer (Bruker). The particle size was determined by using TEM (JEM-2100, Jeol). FTIR spectra were recorded by using Perkin Elmer

spectrophotometer. Analysis of V-I characteristics of nanocomposites was done by using a Four probe set up.

III. Results and Discussion

A. Structural Characterization of ZnS-Graphene Nanocomposites

XRD analysis of ZnS-graphene is shown in Fig. 1 (a). The spectra showed various diffraction peaks at 2θ values 29.04°, 48.7° and 56.8° assigned to the (111), (220), (311) crystal planes of cubic zinc blende phase of ZnS respectively. These values are in agreement with JCPDS file no. 05-0566. Notably, no diffraction peaks for (002) in graphene can be observed in the nanocomposites of ZnS/graphene, which might be due to the low crystallinity and relatively low diffraction intensity of graphene in the nanocomposites of ZnS/graphene.

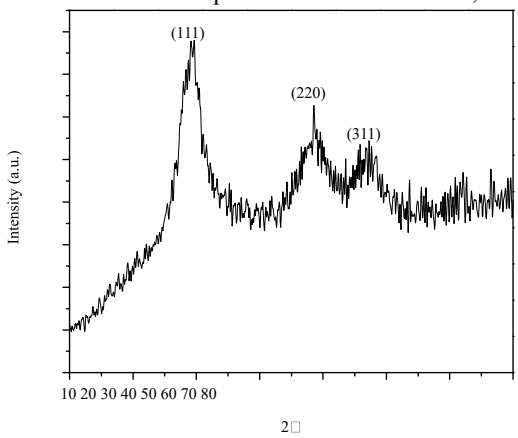

Fig. 1 (a) XRD pattern of ZnS-graphene composites

Fig. 1 (b) SEM image of the ZnS-graphene sample

Fig. 1 (c) EDX spectrum of a ZnS-graphene sample

Fig. 1 (d) TEM image of the ZnS-graphene

Fig. 1 (e) HRTEM image of the ZnS-graphene

Fig. 1 (f) HRTEM image of the ZnS-graphene

Fig. 1 (b) shows the SEM image of ZnS-graphene nanocomposites. These particles show the random aggregation between small particles.

EDX spectrum of ZnS/graphene is shown in Fig. 1 (c). The atomic ratio of ZnS-graphene sample was found to be Zn=54.56%, S=20.12% and C=10.96%.

TEM image of ZnS-graphene is shown in Fig. 1 (d) and HRTEM images are shown in Figs. 1 (e), (f). It can be found that the synthesized ZnS QDs appear as quasi spherical particles present on the graphene sheets. The particle size of ZnS-graphene nanocomposites was found to be 8.4 nm.

B. FTIR Analysis of ZnS-Graphene Nanocomposites

The FTIR spectrum of ZnS-graphene nanocomposites is shown in Fig. 2. The band at 660 cm^{-1} corresponds to Zn-S stretching vibration and band at 1560 cm^{-1} shows absorption of graphene. The band at 1106 cm^{-1} corresponds to C-O-C stretching vibration. The band broadening at 3400 cm^{-1} corresponds to the O-H stretching bond.

C. Electrical Characterization of Zns-Graphene Nanocomposites

The four probe set up was used to measure the voltage– current characteristics of ZnS-graphene nanocomposite. Conductivity of ZnS-graphene QDs was measured by using the equation:

π

The conductivity of the sample was found to be 8.1×10^{-4} S/cm.

IV. Conclusion

ZnS-graphene nanocomposites were prepared successfully by sonochemical method. XRD, SEM, TEM analyses confirm the formation of nanocomposites in cubic phase. From XRD spectra, average size of the nanocrystals was found to be 8.4 nm. TEM analysis reveals bonding of ZnS QDs with graphene sheet. EDX spectrum shows the presence of carbon with zinc and sulphur.urrent-voltage characteristics of ZnS-Graphene

nanocomposite indicates 10^4 times increase in conductivity of nanocomposite as compared to the conductivity of ZnS.

REFERENCES

[1] P. Peumans, S. Uchida, *S.R. Forrest, Efficient bulk heterojunction photovoltaic cells using small-molecular-weight organic thin films, Nature 425 (2003) 158-162.*
[2] R. Liu, Hybrid Organic/Inorganic Nanocomposites for Photovoltaic Cells, Materials 7 (2014) 2747-2771.s
[3] T. Lin, F. Huang, J. Liang, Y. Wang, A facile preparation route for boron-doped graphene, and its CdTe solar cell application, Energy & Environmental Science 4 (2011) 862-865.
[4] Y. Zhou, M. Eck, C. Men, F. Rauscher, P. Niyamakom, S. Yilmaz, I. Dumsch, S. Allard, U. Scherf, M. Kruger, Efficient polymer nanocrystal hybrid solar cells by improved nanocrystal composition, Solar Energy Materials & Solar Cells 95 (2011) 3227-3232.
[5] Z. Pan, H. Zhang, K. Cheng, Y. Hou, J. Hua, X. Zhong, Highly Efficient Inverted Type-I CdS/CdSe Core/Shell Structure QD-Sensitized Solar Cells, ACS Nano 6 (2012) 3982-3991.
[6] C. Gretener, J. Perrenoud, L. Kranz, L. Kneer, R. Schmitt, S. Buecheler, A.N. Tiwari, CdTe/CdS thin film solar cells grown in substrate configuration, Prog. Photovolt:Res. Appl. (2012) doi:10.1002/pip.2233.
[7] L.Y. Chang, R.R. Lunt, P.R. Brown, V. Bulovic, M.G. Bawendi, LowTemperature Solution-Processed Solar Cells Based on PbS Colloidal Quantum Dot/CdS Heterojunctions, Nano Letters 13 (2013) 994-999.
[8] J.N. Freitas, A.S. Goncalves, A.F. Nogueira, A comprehensive review of the application of chalcogenide nanoparticles in polymer solar cells, Nanoscale 6 (2014) 6371-6397.
[9] L.H. Lai, L. Protesescu, M.V. Kovalenko, M.A. Loi, Sensitized solar cells with colloidal PbS–CdS core–shell quantum dots, Phys. Chem. Chem. Phys 16 (2014) 736-742.
[10] R. Ahmed, L. Zhao, A.J. Mozer, G. Will, J. Bell, H. Wang, Enhanced Electron Lifetime of CdSe/CdS Quantum Dot (QD) Sensitized Solar Cells Using ZnSe Core−Shell Structure with Efficient Regeneration of Quantum Dots, J. Phys. Chem. C 119 (2015) 2297-2307.
[11] M.E. Mathew, J.C. Mohan, K. Manzoor, S.V. Nair H. Tamura, R. Jayakumar, Folate conjugated carboxymethyl chitosan–manganese doped zinc sulphide nanoparticles for targeted drug delivery and imaging of cancer cells, Carbohydrate Polymers 80 (2010) 442–448.
[12] F.Y. Shen, W. Que, X.T. Yin, Y.W. Huang, Q.Y. Jia, A facile method to synthesize high quality ZnS(Se) quantum dots for photoluminescence, Journal of Alloys and Compounds 509 (2011) 9105-9110.
[13] X. Wang, H. Hu, S. Chen, K. Zhang, J. Zhang, W. Zou, R. Wang, Onestep fabrication of BiOCl/CuS heterojunction photocatalysts with enhanced visible-light responsive activity, Materials Chemistry and Physics (2015) 1-7.
[14] N.S.N. Jothi, A.G. Joshi, R.J. Vijay, A. Muthuvinayagam, P. Sagayaraj, Investigation on one-pot hydrothermal synthesis, structural and optical properties of ZnS quantum dots, Materials Chemistry and Physics 138 (2013) 186-191.
[15] S. Chaguetmi, F. Mammeri, S. Nowak, P. Decorse, H. Lecoq, M. Gaceur, J.B. Naceur, S. Achour, R. Chtourou, S. Ammar, Photocatalytic activity of TiO2 nanofibers sensitized with ZnS quantum dots, RSC Advances 3 (2013) 2572-2580.
[16] T. Zhao, X. Hou, Y.N. Xie, L. Wu, P. Wu, Phosphorescent sensing of Cr3+ with proteinfunctionalized Mn-doped ZnS quantum dots, Analyst 138 (2013) 6589-6594.
[17] D.I. Son, H.H. Kim, D.K. Hwang, S. Kwon, W.K. Choi, Inverted CdSe–ZnS quantum dots light-emitting diode using low-work function organic material polyethylenimine ethoxylated, J. Mater. Chem. C 2 (2014) 510514.
[18] C. Ippen, T. Greco, Y. Kim, J. Kim, M.S. Oh, C.J. Han, A. Wedel, ZnSe/ZnS quantum dots as emitting material in blue QD-LEDs with narrow emission peak and wavelength tenability, Organic Electronics 15 (2014) 126-131.
[19] M. Mehrabian, K. Mirabbaszadeh, H. Afarideh, Solid-state ZnS quantum dot-sensitized solar cell fabricated by the Dip-SILAR technique, Phys. Scr 89 (2014) 1-8.
[20] H.S. Mansur, A.A.P Mansur, A. Soriano-Araújo, Z.I.P. Lobato, Beyond Biocompatibility: A Novel Approach for the Synthesis of ZnS Quantum Dot-Chitosan Nano-Immunoconjugates for Cancer Diagnosis, Green Chemistry (2015) doi:10.1039/C4GC02072C.
[21] M.R. Kumar, N. Ramamurthy, P. Ambalavanan, Synthesis, structure and optical characterization of zns nanoparticles, International Journal of Current Physical Sciences 1 (2011) 6-9.
[22] J. Kim, C. Park, S.M. Pawar, A.I. Inamdar, Y. Jo, J.Han, J.P. Hong, Y.S. Parkc, D.-Y. Kim, W. Jung, H. Kim, H. Im, Optimization of sputtered ZnS buffer for $Cu_2ZnSnS4$ thin film solar cells, Thin Solid Films 566 (2014) 88–92.
[23] H. Chang and Hongkai Wu, Graphene-based nanocomposites: preparation, functionalization, and energy and environmental applications, Energy Environ. Sci., 6 (2013) 3483–3507.
[24] Y. Yu, Y. Yang, H. Gu, D. Yub, G. Shi, Size-controllable preparation of palladium nanoparticles assembled on TiO2/graphene nanosheets and their electrocatalytic activity for glucose biosensing, Anal. Methods 5 (2013) 7049-7057.
[25] C. Hu , T. Lu , F. Chen, R. Zhang, A brief review of graphene–metal oxide composites synthesis and applications in photocatalysis, Journal of the Chinese Advanced Materials Society 1 (1) (2013) 21-39.
[26] Y. Lei, R. Li, F. Chen, J. Xu, Hydrothermal synthesis of graphene–CdS composites with improved photoelectric characteristics, J Mater Sci: Mater Electron 25 (2014) 3057-3061.
[27] L. Jiang, M. Yao, B. Liu, Q. Li, R. Liu, H. Lv, S. Lu, C. Gong, B. Zou, T. Cui, B. Liu, Controlled Synthesis of CeO2/Graphene Nanocomposites with Highly Enhanced Optical and Catalytic Properties, J. Phys. Chem. C 116 (2012) 11741-11745.
[28] X. Li, X. Wang, L. Zhang, S. Lee, H. Dai, Chemically Derived, Ultrasmooth Graphene Nanoribbon SemiconductorsScience 319 (2008) 1229-1232.
[29] S.K. Kim, D. Yoon, S.-C. Lee, J. Kim, Mo_2C/Graphene Nanocomposite As a Hydrodeoxygenation Catalyst for the Production of Diesel Range Hydrocarbons, ACS Catalysis 5 (6) (2015) 3292–3303,doi:10.1021/acscatal.5b00335.
[30] D. Chen, W. Chen, L. Ma, G. Ji, K. Chang, J.Y. Lee, Graphene-like layered metal dichalcogenide/graphene composites: synthesis and applications in energy storage and conversion, Materials Today 17 (4) (2014) 184-193.
[31] Jaidev, S. Ramaprabhu, Poly(p-phenylenediamine)/graphene nanocomposites for supercapacitor applications, J. Mater. Chem. 22 (2012) 18775–18783.
[32] M. Sookhakian, Y. M. Amin, S. Baradaran , M. T. Tajabadi, A. M. Golsheikh, W. J. Basirun, A layer-by-layer assembled graphene/zinc sulfide/polypyrrole thin-film electrode via electrophoretic deposition for solar cells, Thin Solid Films 552 (2014) 204–211.
[33] L. Scudiero, Y. Shen, M.C. Gupta, Effect of light illumination and temperature on P3HT films, n-type Si,and ITO, Applied Surface Science 292 (2014) 100-106.
[34] P. Ramidi, O. Abdulrazzaq, C.M. Felton, Y. Gartia, V. Saini, A.S. Biris, A. Ghosh, Triplet Sensitizer Modification of Poly(3-hexyl)thiophene (P3HT) for Increased Efficiency in Bulk Heterojunction Photovoltaic Devices, Energy Technol.2 (2014) 604-611.
[35] M.J.M. Wirix, P.H.H. Bomans, H. Friedrich, N.A.J.M. Sommerdijk, G.de With, Three-Dimensional Structure of P3HT Assemblies in Organic Solvents Revealed by Cryo-TEM, Nano Lett. 14 (2014) 2033−2038.
[36] W.-F. Fu, Y. Shi, L. Wang, M.-M. Shi, H.-Y. Li, H.-Z. Chen, A green, low-cost, and highly effective strategy to enhance the performance of hybrid solar cells: Post-deposition ligand exchange by acetic acid, Solar Energy Materials & Solar Cells 117 (2013) 329-335.
[37] S.-H. Choi, H. Song, I.K. Park, J.-H. Yum, S.-S. Kim, S. Lee, Y.-E. Sung, Synthesis of size-controlled CdSe quantum dots and characterization of CdSe–conjugated polymer blends for hybrid solar cells, Journal of Photochemistry and Photobiology A: Chemistry 179 (2006) 135-141.

[38] C.Y. Kwong, W.C.H. Choy, A.B. Djurisic, P.C. Chui, K.W. Cheng, W.K. Chan, Poly(3-hexylthiophene):TiO2 nanocomposites for solar cell applications, Nanotechnology 15 (2004) 1156-1161.
[39] J. Wu, G. Yue, Y. Xiao, J. Lin, M. Huang, Z. Lan, Q. Tang, Y. Huang, L. Fan, S. Yin, T. Sato, An ultraviolet responsive hybrid solar cell based on titania/poly(3-hexylthiophene), Scientific Reports 3:1283 (2013)1-6.
[40] Y. Firdaus, E. Vandenplas, Y. Justo, R. Gehlhaar, D. Cheyns, Z. Hens, M. V. Auweraer, Enhancement of the photovoltaic performance in P3HT: PbS hybrid solar cells using small size PbS quantum dots, Journal of Applied Physics, 116 (2014) 094305.
[41] S.A. Mauger, L. Chang, C.W. Rochester, A.J. Moule, Directional dependence of electron blocking in PEDOT:PSS, Organic Electronics 13 (2012) 2747–2756.
[42] S.B. Dkhil, R. Ebdelli, W. Dachraoui, H. Faltakh, R. Bourguiga, J. Davenas, Improved photovoltaic performance of hybrid solar cells based on silicon nanowire and P3HT, Synthetic Metals 192 (2014) 74-81.
[43] S.D. Oosterhout, M.M. Wienk, S.S. van Bavel, R. Thiedmann, L.J.A. Koster, J. Gilot, J. Loos, V. Schmidt, R.A.J. Janssen, The effect of threedimensional morphology on the efficiency of hybrid polymer solar cells, Nature Materials 8 (2009) 818-824.
[44] E.K. Goharshadi, S.H. Sajjadi, R. Mehrkhah, P. Nancarrow, Sonochemical synthesis and measurement of optical properties of zinc sulfide quantum dots, Chemical Engineering Journal 209 (2012) 113117.
[45] Z. Tang, H. Wu, J. R. Cort, G. W. Buchko, Y. Zhang, Y. Shao, I. A. Aksay, J. Liu, Y. Lin, Constraint of DNA on Functionalized Graphene Improves its Biostability and Specificity, Small, 6(11) (2010) 1205– 1209.
[46] S.-D. Jiang, G. Tang, Y.-F. Ma, Y. Hu, L. Song, Synthesis of nitrogendoped graphene-ZnS quantum dots composites with highly efficient visible light photodegradation, Materials Chemistry and Physics (2014) 1-9.
[47] Z. Jindal, N.K. Verma, Photoluminescent properties of ZnS:Mn nanoparticles with in-built surfactant, J. Mater. Sci. 43 (2008) 65396545.
[48] M.R. Karim, Synthesis and Characterizations of Poly(3-hexylthiophene) and Modified Carbon Nanotube Composites, Journal of Nanomaterials (2012) doi:10.1155/2012/174353.
[49] G.A.H. Wetzelaer, P.W.M Blom, Diffusion-driven currents in organicsemiconductor diodes, NPG Asia Materials (2014) doi:10.1038/am.2014.41.
[50] O. Breitenstein, P. Altermatt, K. Ramspeck, M.A. Green, Jianhua Zhao, A. Schenk, Interpretation of the Commonly Observed I-V Characteristics of C-Si Cells Having Ideality factor Larger Than Two IEEE Xplore (2006) doi: 10.1109/WCPEC.2006.279597.